Proceedings of the Sixth IASTED International Conference
EUROPEAN POWER AND ENERGY SYSTEMS
June 26–28, 2006, Rhodes, Greece

SYNCHRONIZATION OF DFIG OUTPUT VOLTAGE TO UTILITY GRID IN WIND POWER SYSTEM

Ahmed G. Abo-Khalil [1], Dong-Choon Lee [2], Seung-Pyo Ryu [3]
Dept. of Electrical. Eng. Yeungnam Univ., 214-1, Daedong, Gyeongsan, Gyeongbuk, Korea
E-mail [2] : dclee@yu.ac.kr, Tel: +82-53-810-2582 , Fax: +82-63-810-4767
Electro-Mechanical Research Institute, Hyundai Heavy Industry Co., Ltd, Gyeongki, Korea [3]

ABSTRACT
This paper presents a new synchronization algorithm for grid connection of a doubly fed induction generator (DFIG) in a variable speed wind generation system. Stator flux-oriented vector control with back-to-back PWM converters in the DFIG rotor circuit is used for synchronization process. By controlling the rotor d-axis current, the magnitude of the stator EMF is adjusted to be equal to the grid voltage. PLL circuit is used to compensate for the phase shift between the stator EMF and the grid voltage. By controlling the turbine pitch angle, the generator speed is determined to adjust the stator frequency to be equal to the grid. Simulation results using PSCAD show a smooth synchronization and fast dynamic responses.

KEY WORDS
Wind power generation, DFIG, synchronization, grid utility

1. INTRODUCTION
It is well known that wind power generation using a variable-speed constant-frequency (VSCF) scheme produces electricity over a wide range of wind speeds, thus having a high energy capture capability. One commonly used VSCF scheme employs a doubly-fed wound-rotor induction generator (DFIG) using an ac/dc/ac PWM converter in the rotor circuit [l], [2]. The DFIG can supply power at constant voltage and constant frequency while the rotor speed varies. This makes the DFIG suitable for variable speed wind power generation. The main advantages of this system are the decoupled control of active and reactive power and the reduced rating of power converter (25-30%). The DFIG using back-to-back PWM converters for the rotor circuit has been well established in wind generation applications. When used with a wind turbine, it offers several advantages compared with fixed speed generators. These advantages, including speed control and reduced flicker, are primarily achieved by controlling the voltage source converter, with its inherent four-quadrant active and reactive power capabilities [3], [4].

As shown in Fig. 1, the stator of the DFIG is connected through SW 3 to the balanced three-phase grid and the rotor side is fed via the back-to-back IGBT voltage-source converters with a common dc bus. The ac-dc converter controls the power flow between the dc bus and the rotor side and allows the system to be operated in sub-synchronous or super-synchronous speed. The active power is generated based on the wind speed value and wind turbine characteristics while the reactive power command is determined as a function of the desired reactive power converter compensation. The vector control strategy of the power converter is based on the stator-flux oriented control which allows a decoupled control of generator torque and rotor excitation current. The control system makes it possible to improve dynamic behavior of the wind turbine, resulting in the reduction of the drive train stress and electrical power fluctuations, and increasing energy capture [5], [6].

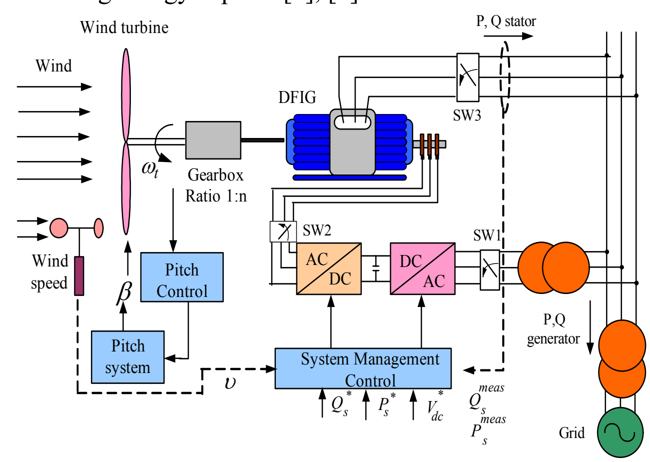

Fig. 1 Basic configuration of DFIG wind turbine system

The DFIG operation and control have been intensively investigated so far. On the other hand, only a few papers have handled the DFIG control during the synchronization process. There are two control schemes for DFIG synchronization published. One method is based on direct torque control (DTC) [7], and the other is based on the field oriented control (FOC) [8].

This paper describes soft and fast synchronization of the DFIG to the grid as well as independent control of active and reactive power of the generator using the stator flux-oriented control at normal operation. During the generator synchronization process, the turbine pitch angle controller adjusts the speed closely to the synchronous speed to make it sure that the stator frequency is the same as that of the grid. The magnitude of stator EMF is controlled by adjusting the rotor flux and the phase shift between the stator and grid voltages is compensated by PLL circuit. The wind turbine control system are developed using PSCAD software.

2. SYNCHRONIZATION CONTROL OF DFIG

2.1 Wind Turbine Characteristics

The wind turbine can be characterized by its $C_p - \lambda$ curve (as shown in Fig. 2), where the tip-speed ratio λ is defined as the ratio between the linear speed of the tip of the blade to the wind speed.

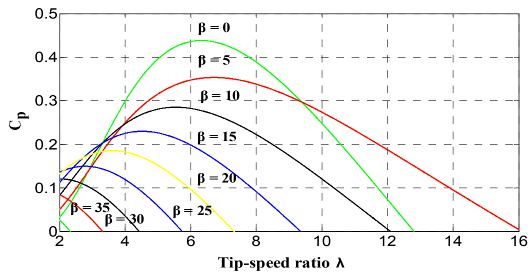

Fig. 2 Variation of power conversion coefficient with pitch angle β

It is shown that the power coefficient C_p varies with the tip-speed ratio. It is assumed that the variable wind turbine is operated at high C_p values most of the time. In a fixed-frequency application, the rotor speed of the induction generator varies by a small percentage (based on the slip) above the synchronous speed while the speed of the wind may vary over a wide range. The power captured by the wind turbine may be written as (1)

$$P_m = \frac{1}{2}\rho\pi R^2 \upsilon^3 C_p(\beta,\lambda) \tag{1}$$

and the tip-speed ratio is defined as

$$\lambda = \frac{\omega_t R}{\upsilon} \tag{2}$$

where,

ρ : specific density of air [kg/m^3];

υ : wind speed [m/s];

R : radius of the turbine blade[m];

ω_t : turbine speed;

C_p : coefficient of power conversion;

β : pitch angle.

From (1), it is apparent that the power production from the wind turbine can be maximized if the system is operated at maximum C_p.

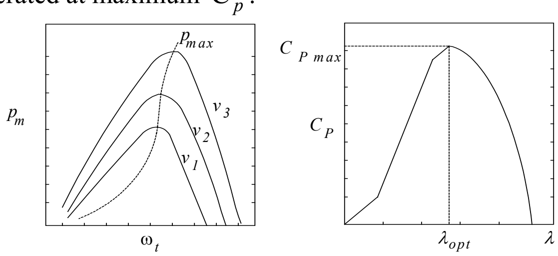

(a) (b)

Fig. 3 Characteristic curves of wind blades
(a) Output power versus rotational speed
(b) Power conversion coefficient versus tip-speed ratio

Fig. 3(a) shows that the power captured in turbine blades is a function of the rotational speed and that it is maximum at the particular rotational speed. Fig. 3(b) shows that the value of C_p is a function of λ and it is maximum at the particular λ_{opt}. Hence, to fully utilize the wind energy, λ should be maintained at λ_{opt}, which is determined from the blade design. Then, from (1),

$$P_{\max} = 0.5\rho\pi R^2 C_{p\max}\upsilon^3 \tag{3}$$

The reference speed of the generator is determined from (2) as once the wind velocity υ is measured, the reference speed for extracting the maximum power point is obtained from (4).

$$\omega_t^* = \frac{\lambda_{opt}}{R}\upsilon \tag{4}$$

Once the wind velocity υ is measured, the reference speed for extracting the maximum power point is obtained from (4).

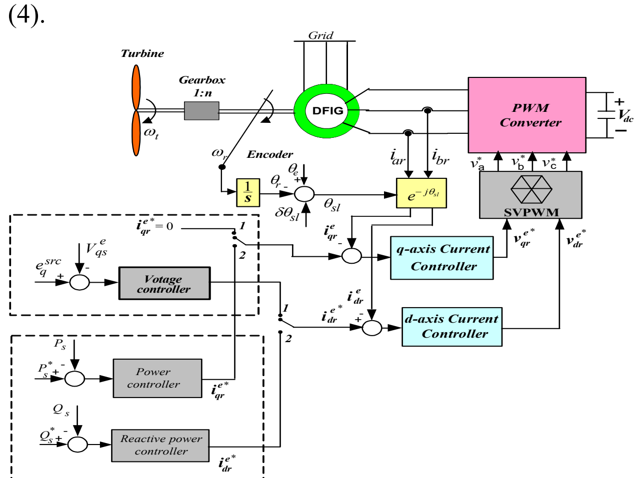

Fig. 4 Control block diagram of DFIG system

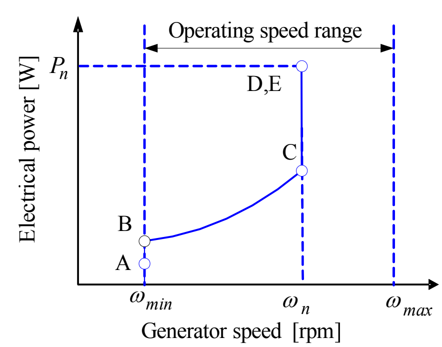

Fig. 5 Operating modes of wind turbine

2.2 Control of Rotor-side

Fig. 4 shows the schematic of the DFIG wind turbine configuration and its simplified control scheme. The stator of the DFIG is connected to the utility grid. The back-to-back PWM converters provide a bidirectional power-flow control thereby enabling the DFIG to operate either in subsynchronous $(\omega_r < \omega_s)$ or in supersynchronous modes ($\omega_r > \omega_s$). In both modes the stator active power is generated from the DFIG and delivered to the grid. On the other hand, the rotor active power is either supplied to the machine in the subsynchronous mode or delivered to the grid in the supersynchronous mode [9]. The stator active power is controlled directly assuming that a maximum generator power is known from the optimum generator speed value. The operating curve of the wind turbine, which is applied to most modern wind turbines [5], is illustrated in Fig. 5. This curve is characterized by four sections as follows; A~B for the rotor speed which is less than the minimum angular speed for optimum operation, B~C for an optimal characteristic curve given by $P_{opt} = K_{opt}\upsilon^3$ in between the cut-in speed and the rated speed, C~D for a constant speed characteristic up to the rated power, and D~ E for a constant power characteristic beyond the speed limit followed by a blade pitch control action for high wind speed [10], [11].

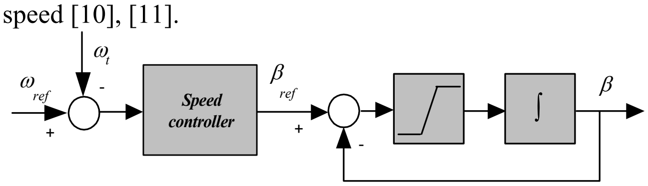

Fig. 6 Block diagram of pitch angle control

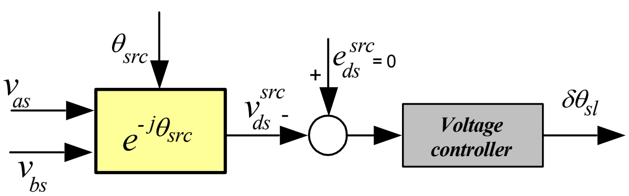

Fig. 7 Phase difference compensation for synchronization

The stator power reference P^* of the DFIG is used as the reference value for the power control loop. In the inner current control loop, the stator-flux vector position is used to establish a reference frame that allows q-axis components of the rotor current to be controlled. As the reference rotor current components are in stator-flux oriented coordinates, these must be transferred to the same reference frame as the rotor current vector of the DFIG. This is achieved by rotating the rotor reference current vector by an angular position θ_{sl}. Due to the rotor speed variation, θ_{sl} is updated at every sample interval. Once the reference frame for both the reference and measured current vectors are conformed, simple proportional plus integral (PI) regulators can be used to control the d- and q-components of the rotor current.

Adjustment of the q-axis component of the rotor current controls either the stator-side active power or the developed torque of the DFIG.

$$\begin{aligned} P_s &= \frac{3}{2}(v_{qs}i_{qs} + v_{ds}i_{ds}) = \frac{3}{2}\cdot v_{qs}i_{qs} \\ &= -\frac{3}{2}\cdot\frac{L_m}{L_s}\cdot v_{qs}i_{qr} \end{aligned} \tag{5}$$

$$\begin{aligned} T_e &= \frac{3}{2}\cdot\frac{P}{2}\cdot\frac{L_m}{L_s}(\lambda_{qs}i_{dr} - \lambda_{ds}i_{qr}) \\ &= -\frac{3}{2}\cdot\frac{P}{2}\cdot\frac{L_m}{L_s}\cdot\lambda_{ds}i_{qr} \end{aligned} \tag{6}$$

where P_s is the stator power, v_{qs}, v_{ds}, i_{qs} and v_{ds} are the d-q stator voltage and current components, L_s and L_m are stator and magnetizing inductances, $\lambda_{ds}, \lambda_{qs}$ are the d-q axis stator flux components and i_{dr}, i_{qr} are the d-q axis rotor current components.

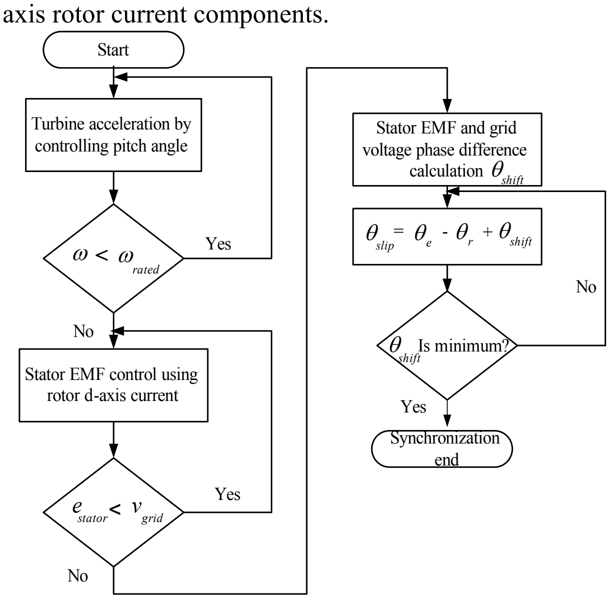

Fig. 8 Sequence of synchronization

Regulating the d-axis rotor current controls directly the stator-side reactive power as shown in Fig. 4.

$$\begin{aligned} Q_s &= \frac{3}{2}(v_{qs}i_{ds} - v_{ds}i_{qs}) = \frac{3}{2}\cdot v_{qs}i_{ds} = \frac{3}{2}\cdot v_{qs}\left(\frac{\lambda_{ds} - L_m i_{dr}}{L_s}\right) \\ &= \frac{3}{2}\cdot\frac{L_m}{L_s}\cdot v_{qs}\left(\frac{v_{qs}}{L_m\omega_e} - i_{dr}\right) = \frac{3}{2}\cdot\frac{L_m}{L_s}\cdot v_{qs}(i_{ms} - i_{dr}) \end{aligned} \tag{7}$$

2.3 Synchronization Process

The connection of a DFIG to a utility grid requires that the voltage, frequency and phase angle of both parts be matched exactly before the generator is connected to the grid. The synchronization control process can be accomplished by controlling the turbine pitch angle and the generator d-q axis currents. At standstill, rotor blades are in a feathering position and the generator is disconnected from the grid. In the synchronization stage, the turbine is driven by the wind but still disconnected from the grid and the rotor speed is controlled by changing the pitch angle. The speed controller, shown in Fig. 6, accelerates the turbine until it reaches the speed required for synchronization. At this moment the stator frequency will be about the same as that of the grid. The reference torque component of the rotor current i_{qr} is zero as the generator is still running at no-load and the d-axis component of the stator EMF is zero.

By adjusting the rotor d-axis current, the amplitude of the stator EMF can be the same as the grid voltage. Even slightly different frequencies will cause the phase difference between the two voltages as shown in Fig. 8. In the right part of the block in Fig. 6, the d-axis component of the stator EMF is compared with the grid voltage and the error value is controlled using PI controllers until the two values become the same. It should be noted that the currents in the flux-oriented frame are constant and consequently the inductor voltage are zero. Also, the stator-flux orientation is defined by aligning the reference frame to the stator flux axis. It means that $\lambda_{qs} = v_{ds} = 0$.

To compensate for the phase difference between the stator EMF and grid voltage, the phase difference compensation component is added to the calculated slip angle. Finally, after the synchronization condition is achieved, the stator-side contactor is closed, and the generator is connected to the grid. After synchronization, the controller must dynamically regulate the active and reactive power of generator as discussed in the previous section.

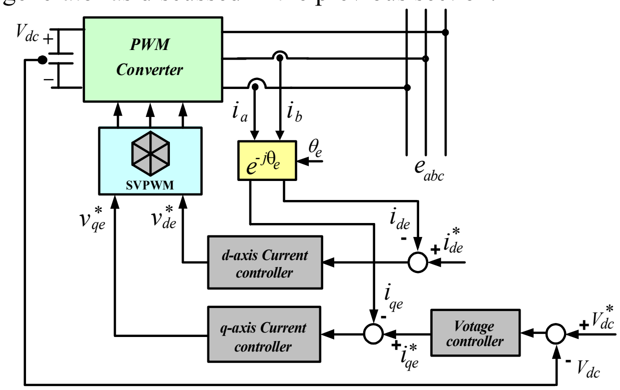

Fig. 9 Control block diagram of grid-side converter

The disconnecting sequence of the DFIG from the grid is reverse to the connecting process. When disconnected from the grid, the generator is gradually unloaded, and while approaching to no load condition the generator is disconnected from the grid as shown in Figs. 4 and 7.

2.4 Control of Grid-side Converter

The function of the grid-side converter is to keep the dc-link voltage constant regardless of the magnitude and direction of the rotor power [12]. If a vector-control method is applied, with a reference frame oriented along the grid voltage vector position, an independent control of the active and reactive power for the grid-side is guaranteed. Fig. 9 shows a block diagram of the grid-side converter control. The PWM converter is current-regulated, where the q-axis current controls the dc-link voltage and the d-axis current control can be used for the reactive power control of the grid.

3. SIMULATION RESULTS

Using PSCAD, the proposed control system has been simulated to verify its validity for the smooth and fast synchronization. The ratings and parameters of the DFIG are given in Table I while the turbine parameters are given in Table II. At t=0, the inverter contactor is closed and the dc link voltage is controlled to the reference value. Speed, torque, rotor and stator currents are all zero because the rotor and stator are open-circuited as shown in Fig. 10. Next, the rotor contactor is closed and the synchronization process starts. By adjusting the turbine speed closed to the synchronous speed (1800 rpm), a stator frequency equal to the grid frequency can be obtained. At the same time, the d-axis current increases to increase the stator EMF until the stator EMF and the grid voltage are equal. Zero phase-difference is obtained by compensating for the phase difference between the two voltages. As shown in Fig. 11, the EMF was zero before starting synchronization procedure, then the EMF magnitude, frequency, and phase difference are adjusted with respect to the grid values. It is noticeable that the synchronization process takes almost two cycles, which means that the synchronization control is fast. After satisfying the synchronization conditions, the stator contactor is closed and the generator supplies the grid with the power corresponding to the wind speed.

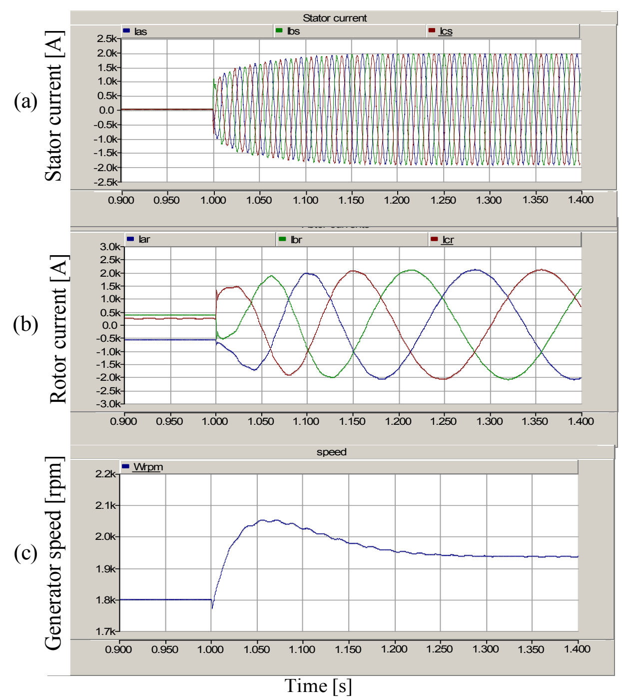

Fig. 10 Generator performance at synchronization process

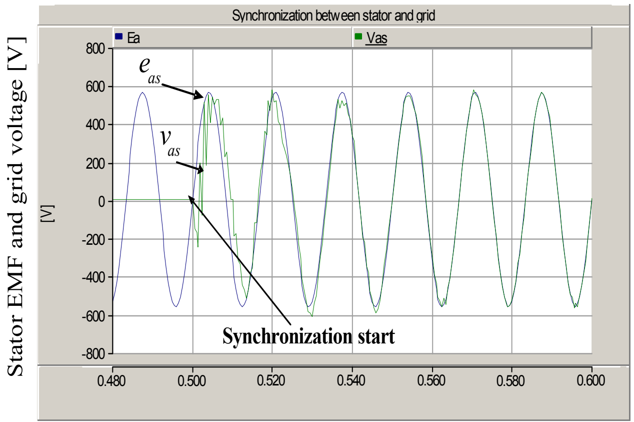

Fig. 11 Stator voltage v_{as} and grid voltage e_{as}

The generator active power is zero before synchronization, and then the power reference is adjusted to extract the maximum power based on the wind speed value as shown in Fig. 12(a). The stator reactive power is controlled to be zero during all modes. As the active power increases the generator torque also increases as shown in Fig. 12(c).

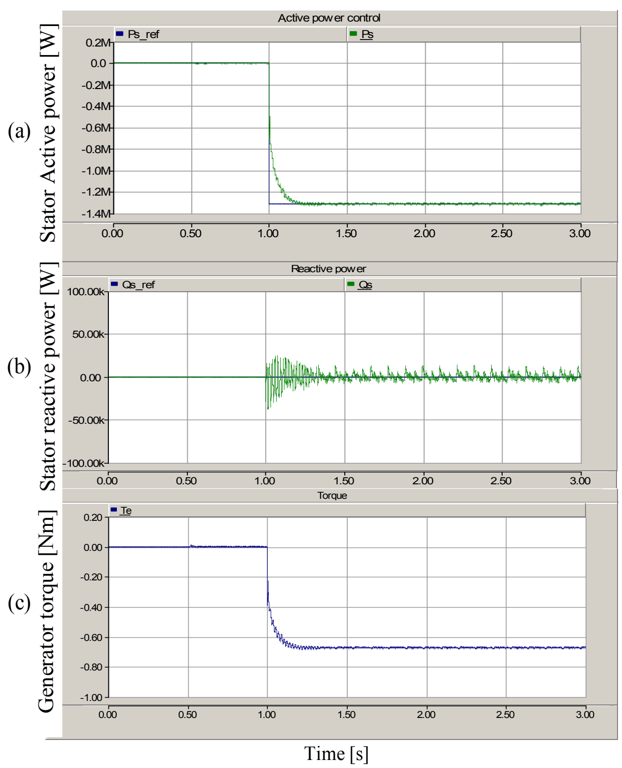

Fig. 12 Stator active, reactive power and generator torque

After a fault occurs in the external networks, the following control steps are performed:

1. Disconnecting the stator and grid are kept connected.
2. Reactivate the pitch angle controller to reduce the aerodynamic power.
3. After fault clearing, the synchronization steps can be applied to recover the generator voltage.

In Fig. 13, the fault occurs after 2 [s], then the aforementioned steps are performed to resynchronize the generator. The stator current during the disconnection is zero, while the rotor current is equal to the magnetizing current. The stator active power is adjusted to the maximum power value during normal operation and then set to zero during faults as shown in Fig. 13(c).

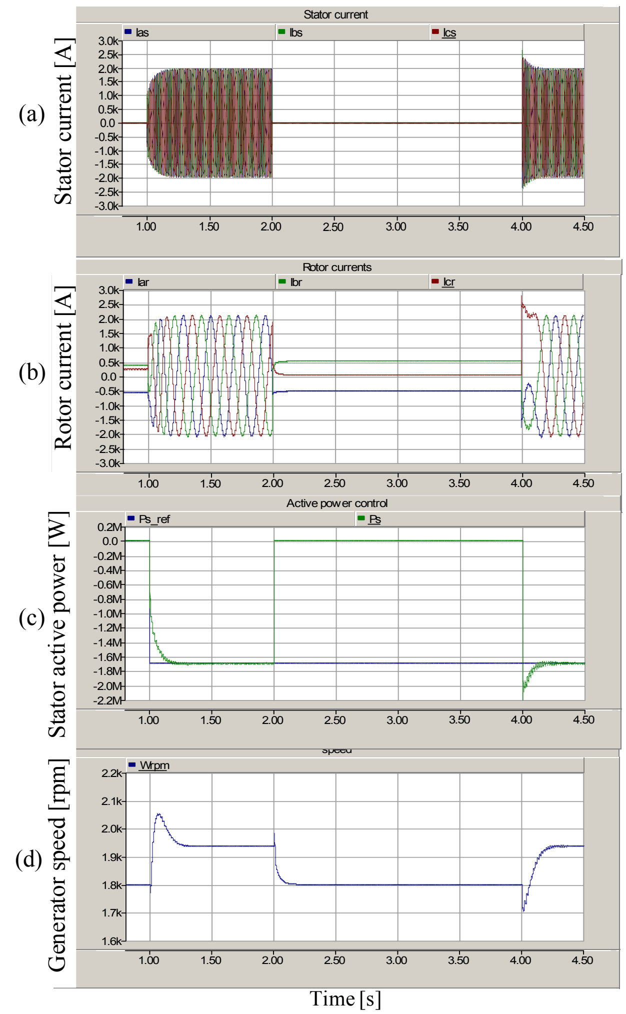

Fig. 13 Generator performance at different control modes

The generator speed is determined by the operating active power and is adjusted to the synchronous speed during faults by the pitch angle controller as shown in Fig. 13(d). After fault clearing, the generator power and speed are controlled to extract the maximum power.

It is noticeable that the system is reliable and fast to achieve synchronization as well as good running performance.

4. CONCLUSION

In this paper, a synchronization scheme for stator flux-oriented DFIG control systems to the utility gird has been proposed. The pitch angle controller adjusts the turbine speed at the required value for equal frequency. The stator voltage is generated to be equal to the grid voltage by adjusting the rotor d-axis current. The voltage phase difference is compensated using the d-axis voltage component of both sides. The synchronization process is independent of the wind speed, so if the wind speed range between the cut-in and cut-out speed, the pitch angle controller adjusts the angle to the proper value. The proposed synchronization algorithm gives smooth and fast synchronization, which enables the system to be reclosed quickly after grid fault clearing. PSCAD simulation has verified that the proposed synchronization algorithm is effective.

APPENDIX

The specifications of the doubly-fed induction generator used for simulation are listed in Table I.

Table 1. Parameters of DFIG

Parameters	Value
Rated power	2[MW]
Rated line voltage	690[V]
Stator resistance	0.00488 [p.u.]
Rotor resistance	0.00549 [p.u.]
Stator leakage inductance	0.09241 [p.u.]
Rotor leakage inductance	0.09955 [p.u.]
Mutual inductance	3.95279 [p.u.]
Number of poles	4
Grid frequency	60[Hz]
Moment of inertia	4800 kg.m^2

Table 2. Parameters of Turbine Blade Model

Parameters	Value
Blade radius	40 [m]
Max. power conv. coeff.	0.45
Optimal tip-speed ratio	7
Cut-in speed	4 [m/s]
Rated wind speed	12 [m/s]
Gear ratio	80
Moment of inertia	$1.26{\cdot}(10)^7$ [kg.m^2]

ACKNOWLEDGEMENTS

This work has been supported by the KEMCO (Korea Energy Management Corporation) under project grant (2004-N-WD12-P-06-3-010-2005).

REFERENCES

[1] L. Zhang, C. Watthansarn, and W. Shehered, "A matrix converter excited doubly-fed induction machine as a wind power generator," *IEEE IECON Conf. Proc*., vol. 2, pp. 906 - 911, Nov. 2004.

[2] P. Cartwright, L. Holdsworth, J. B. Ekanayake, and N. Jenkins, "Co-ordinated voltage control strategy for a doubly-fed induction generator (DFIG)-based wind farm," *IEE proc. on Generation, Transmission and Distribution*, Vol. 151, no. 4, pp. 495-502, Jul 2004.

[3] R. Pena, J. C. Clare, and G. M. Asher, "A doubly fed induction generator using back-to-back PWM converters supplying an isolated load from a variable speed wind turbine," *IEE proc. on Electric Power Appl*., vol. 143, pp. 380-387, 1996.

[4] T. Sun, Z. Chen, and F. Blaabjerg, "Transient analysis of grid-connected wind turbines with DFIG after an external short-circuit fault," *NORDIC WIND POWER CONFERENCE*, 1-2 MARCH, 2004, pp. 1-7.

[5] Y. Lei, A. Mullane, G. Lightbody, and R. Yacamini, "Modeling of the wind turbine with a doubly-fed induction generator for grid integration studies," *IEEE Trans. Energy Conv.*, vol. 21, No. 1, March 2006, pp. 257 – 264.

[6] S. A. Gomez and J. L. R. Amenedo, "Grid synchronisation of doubly fed induction generators using direct torque control," *IEEE IECON Conf. Proc.,* vol. 4, 2002, pp. 3338-3343.

[7] R. Chedid, F. Mard, and M. Basma, "Intelligent control of a class of wind energy conversion systems," *IEEE Trans. Energy Conv.,* 1999, 14, (4), pp. 1597-1604

[8] G. Yuan, J. Chai, and Y. Li, "Vector control and synchronization of doubly fed induction wind generator system", *The 4th International PEMC Conf.*, Vol. 2, pp. 886-890, 2004.

[9] B. Boukhezzar and H. Siguerdidjane, "Nonlinear control of variable speed wind turbines without wind speed measurement," *Proc. of IEEE CDC-ECC'05*, 44th , Dec. 2005, pp.3456 – 3461.

[10] T. Thringer and J. Linders, "Design criteria of variable speed wind turbines with doubly fed induction generator," *Proc. European Wind Energy Conf.*, vol. 8, No. 3, 2001, pp. 1116-1119, July. 2001.

[11] T. Thiringer, "Power quality measurements performed on a low-voltage grid equipped with two wind turbines", *IEEE Trans. Energy Conversion*, vol. 11, pp. 601-606, Sept. 1996.

[12] David Parker, "Computer based real-time simulator for renewable energy converters," *IEEE Proc. International Workshop on Electronic Design, Test and Applications*, Jan. 2002, pp. 280-284.